

reduction in lateral load resistance of around 10%. The column otherwise behaved in a ductile manner, generally consistent with a deformation-controlled Type 1 or 2 backbone curve.

Newell (2008) tested nine seismically compact W14 columns at the University of San Diego. The section types of the specimens were W14x132, W14x176, W14x233 and W14x370. The slenderness ( $L/r_y$ ) for these specimens varied from 46 to 53. Each of the columns was subjected to a gravity load demand of  $0.15P/P_{yn}$ . The total axial load demand varied with time during the test with target maximum axial load ratios of: 0.35, 0.55 and 0.75  $P/P_{yn}$ . The axial load demand was varied throughout the tests with the intent of simulating axial load demands from a seismic event. The test results indicated that the columns were capable of sustaining large plastic rotation demands of 6.5% to 8.5%. These limits were defined at the point when the lateral load resistance reduced by 10%.

MacRae (1989) tested eight I-section columns at the University of Canterbury. This research was performed with the specific intent of verifying the suggested axial load limit ( $P/P_y$ ) of 0.5 suggested by Popov 1975. Specimens C0, C3, C4, C5, C6, C7, C8 were loaded to axial load ratios of 0, 0.3, 0.4, 0.5, 0.6, 0.7, 0.8. One specimen (CA) was loaded with a varying axial load of 0 to 0.6 with a 0.3 gravity component. The specimens were eight identical columns with slenderness ratio ( $L/r_y$ ) of 17, web slenderness ratio ( $h/t_w$ ) of 29 and a flange slenderness ratio ( $b/t$ ) of 9.2. The plastic rotation capacity of the specimens varied from 3.7% at zero axial load to 1.1% at an axial load ratio of 0.80. All specimens reached a displacement ductility capacity of at least 8.

Uang (2015) tested a matrix of five W24 sections that varied from W24x55 to W24x176. These specimens were investigated under three levels of axial load,  $C_a = 0.2, 0.4$  and  $0.6$ . The slenderness ratios ( $L/r_y$ ) for the columns varied from 161 to 71. The web slenderness ( $h/t_w$ ) varied from 60 to 34 while the flange slenderness ( $b/t$  ratios ranged from 6.9 to 4.8. The testing concluded that the slenderness ratios for local buckling and lateral torsional buckling had a significant effect on the failure modes of the columns. Few of the specimens reached a plastic rotation capacity of 3%.

Brownlee tested seventeen column specimens with axial load ratios ranging from 0 to 0.70 with the purpose of comparing results to NZS 3404 acceptance criteria. The slenderness ratio of the specimens varied from between 43 and 73. Web and flange compactness varied between 30 to 90 and 8.4 to 14.7 respectively. Plastic rotation capacities of columns tested with and axial load ratio of 0.7 varied from approximately 0.5% to 1.4%. Brownlee concluded that NZS acceptance criteria are conservative for axial loads less than 0.5 and that satisfactory behavior at higher axial loads can be achieved with stocky members.

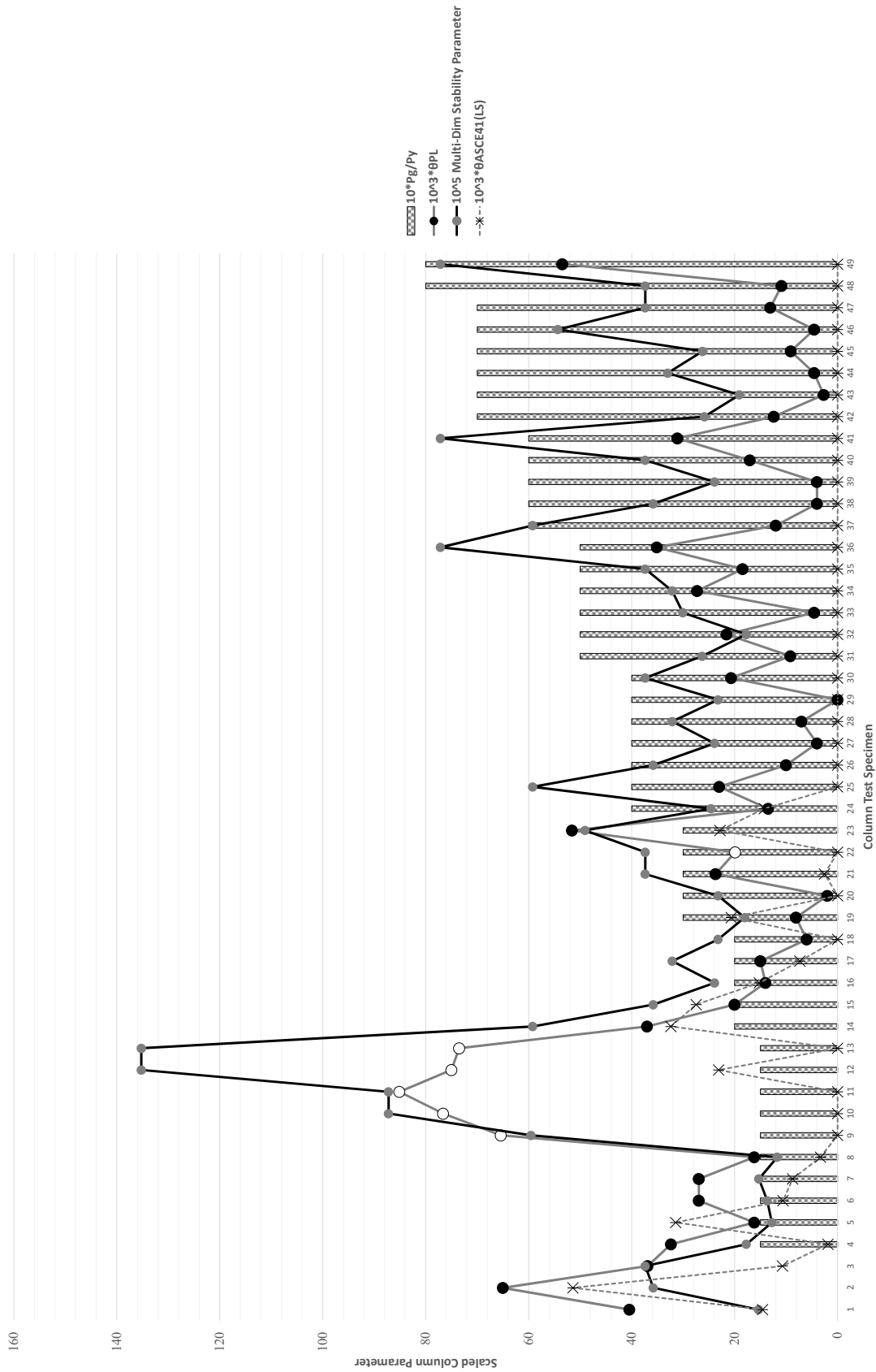


Figure 6 – Plastic Rotation Capacity vs. Multi-Dimensional Stability Parameter & ASCE41

Based on the research presented above it is clear that plastic rotation capacity  $\theta_{PL}$  is a function of the axial load ratio ( $P/P_y$ ), the compactness of the section ( $h/t_w$ ,  $b/2t_f$ ) and slenderness ( $L/r_y$ ). As a consistent relationship between any of the above individual parameters and plastic rotation capacities cannot be derived, the Authors have created a parameter that helps illustrate the combined influence of slenderness and compactness on plastic rotation capacity. Figure 6 plots a multi-dimensional stability parameter that combines column slenderness, flange and web compactness against the testing performed by Popov (1975), MacRae (1989), Brownlee (1994), Newell (2008) and Uang (2015). The multi-dimensional parameter is derived by taking the inverse of the summation of the slenderness ratio plus the product of flange and web compactness.

Figure 6 is presented with increasing axial load from left to right. Note that all parameters have been multiplied by a scalar for ease of comparison. For example, a plastic rotation of 0.06 radians is multiplied by 1000 and reported as 60. The plastic rotation reported is taken at the point on the hysteresis where the specimen has had a reduction in lateral resistance of 10%. For comparison the plastic deformation capacity of the specimens using the ASCE 41 Life Safety Criteria with  $P/P_{cl}$  are provided. Where ASCE 41 gives zero plastic rotation capacity the ratio  $P/P_{cl}$  is close to or exceeds 0.5.

Several of the specimens presented were tested with varying (transient) axial load which is considered more representative of seismic demands. The plastic rotation values for these specimens are shown as hollow data points in Figure 6. The Newell (2008) test specimens were subjected to a gravity load demand of  $P_g/P_y$  of 0.15 but included a transient axial load as high as 0.75. As can be seen the plastic rotation capacity did not vary significantly between the specimens. MacRae (1989) tested one specimen with a gravity load demand ( $P_g/P_y$ ) of 0.30 and a transient component that varied from 0 to approximately 0.60. The MacRae specimen indicated a significant reduction in plastic rotation capacity relative to Newell's tests which suggests that the plastic rotation capacity is more strongly related to the permanent gravity load than the transient seismic load. This relationship is also referenced in the commentary of section 12.8.3.1 of NZS 3404.

From review of Figure 6 it is clear that there is a strong dependence of plastic rotation capacity with web slenderness, flange slenderness and the slenderness of the specimen. For the majority of specimens, the plastic rotation is directly related to the multi-dimensional stability parameter with additional dependence on axial load.

Prior to proposing changes to the column evaluation criteria in Table 9-6 it is important to note that the case studies (Building A, B and C) presented in this paper are not isolated archetypes solely defined by the Authors. NIST Technical Note 1863-1, Volume 1 summarizes the performance based evaluation of several archetype moment frame buildings. The analytical results in the study indicate that Special Moment Resisting Frames designed in accordance with ASCE 7, and its reference standards, have difficulty satisfying the ASCE 41 BSO performance objective. The study concludes that a

significant number of the columns in the archetype buildings fail to meet the force-controlled acceptance criteria stipulated in ASCE 41. The study recommends that  $P_{ce}$  be used instead of  $P_{cl}$  for the evaluation of force-controlled behavior. The technical note goes on to recommend additional research to justify updated interaction equations within ASCE 41 to be more in line with “highly vetted design standards.” The Authors presume this is a reference to AISC 360. Many other recommendations are made but are less relevant to the column topic discussed herein.

## PROPOSED CHANGES TO ASCE 41 ACCEPTANCE CRITERIA

As can be seen from the analysis performed on the subject buildings numerous steel columns are classified as force-controlled when evaluated against ASCE 41-13 acceptance criteria. Based on review of the research presented, columns with high axial loads have dependable plastic rotation capacity whilst maintaining capacity to resist imposed vertical and lateral forces, and thus should not be arbitrarily classified as force-controlled. Accordingly, several proposed changes to the AISC 41-13 column modeling and acceptance criteria are presented below.

### Adjust Yield Rotation

As discussed earlier, Table 9-6 outlines the plastic rotation capacities allowed by ASCE 41-13, these capacities are reported as a multiple of the yield rotation. There are two issues with this approach. First, Equation 9-2 of ASCE 41-13 provides the yield rotation based on Euler Bernoulli beam theory and thus does not account for the contribution of shear deformation to the yield rotation. Shear deformation of the column can be a significant component of column deformation prior to yield, Newell (2008). The yield point is determined by the strength interaction surface, which varies as a function of axial and flexural demand, not yield rotation which is estimated for a given axial or flexural demand; however, per ASCE 41-13, estimated yield rotation is used to determine the plastic rotation capacity of the element. The Authors review of column deformation demands from the case study buildings concurs with Newell’s finding that the yield equation for columns in ASCE 41 should be adjusted to include shear deformation.

Equations 9-27 through 9-32 contained in ASCE 41-13 provide a yield rotation that includes both the flexural and shear deformation and are repeated below for reference. Newell (2008) has suggested alternate (but similar) equations in his research however these are referenced as they are already contained in ASCE 41. These equations were intended to be used for Eccentrically Brace Frame link but can be used for columns as they capture all imposed deformation demands compared with the current provisions which neglect shear deformation.

$$K_e = \frac{K_s K_b}{K_s + K_b} \quad (\text{Eqn 9-27})$$

Where,

$$K_s = \frac{GA_w}{e} \quad (\text{Eqn 9-28})$$

$$K_b = \frac{12EI_b}{e^3} \quad (\text{Eqn 9-29})$$

Where,

$A_w = (db - 2tf)$

$e =$  length of element

$G =$  shear modulus

$K_e =$  stiffness of the element

$K_b =$  flexural stiffness

$K_s =$  shear stiffness

$$\theta_y = \frac{Q_{CE}}{K_e e} \quad (\text{Eqn 9-30})$$

The strength of the element  $Q_{CE}$  is calculated as follows:

$$\text{If } e \leq \frac{1.6M_{CE}}{V_{CE}} \text{ then } Q_{CE} = 0.6F_y A_w \quad (\text{Eqn 9-31})$$

$$\text{If } e > \frac{2.6M_{CE}}{V_{CE}} \text{ then } Q_{CE} = \frac{2M_{CE}}{e} \quad (\text{Eqn 9-32})$$

When the element length is between the limits of equation 9-31 and 9-32 then linear interpolation is used. The strength  $Q_{CE}$  is adjusted for axial load by reducing  $M_{CE}$  by one minus the axial load ratio. In most instances the columns of buildings A, B and C are controlled by flexure but in some instance inclusion of shear deformation has a significant effect. Newell (2008) noted that the inclusion of shear deformation on yield will increase the yield rotation from equation 9-2 from 10% to 50%.

The column acceptance criteria in Table 9-6 trend toward and become equal to the beam acceptance criteria as the axial load ratio reduces below 0.15. Similarly, the EBF link acceptance criteria trend toward and become equal to the beam acceptance criteria as the link element becomes controlled by flexure.

#### Adjust Compactness Limits

The compactness limits placed on the plastic rotation capacities in Table 9-6 are based on AISC 341-97 and 2<sup>nd</sup> edition of the Manual of Steel Construction. These limits should be adjusted to match AISC 341-10 values with  $\lambda_{hd}$  aligned with the (a) plastic rotation limits in Table 9-6 and  $\lambda_{md}$  aligned with the (b) plastic rotation limits.

### Adjust Force-controlled Limit

The onset of force-controlled behavior is defined by ASCE41 at an axial load ratio of  $P/P_{cl}$  equal to 0.5 where  $P_{cl}$  is defined as the lower bound compressive strength of the column. FEMA 273, the predecessor to ASCE 41, defined the onset of force-controlled behavior at  $P/P_{ce}$  not  $P/P_{cl}$ . The change to  $P/P_{cl}$  occurred when FEMA 273 transitioned to FEMA 356 without explanation in the commentary.

The research presented indicates that steel columns are deformation controlled elements and do not exhibit Type 3 (Figure 7-4, ASCE 41) force-controlled behavior even at very high axial loads. Steel columns should generally be classified as deformation controlled elements. However, columns with high un-factored gravity load demands ( $P_g/P_{ce} > 0.6$ ) may have been under designed for gravity load. Thus, for columns with  $P_g/P_{ce} > 0.60$  it is recommended that plastic rotation capacities be set to zero (ie force-controlled) to protect these columns from potential overloading under combined gravity and seismic load.  $P_g$  is defined as the dead load plus 25% of the gravity load for application in ASCE 41-13 evaluations.

### Adjust Plastic Rotation Limits

As demonstrated in the research presented and the performance of the case study buildings, the plastic rotation capacities for columns reported in Table 9-6 of ASCE 41 need to be adjusted to avoid overly conservative performance assessments and retrofit designs. The current acceptance criteria are under conservative for columns with low axial load and overly conservative for columns with high axial loads as illustrated in research by Newell. The plastic rotation limits should be adjusted so they are a function of:

1. **Section Compactness** – The compactness requirements of Table 9-6 of ASCE 41 should be aligned with current code requirements of AISC 341-10.
2. **Axial Load Ratio** – The axial load ratio on which the plastic limits are based should be changed from  $P/P_{cl}$  to  $P_g/P_y$  as this is consistent with the majority of the testing performed. Further, this change is consistent with the observations made earlier in this report and noted in NZS 3404 that the plastic rotation capacity is more dependent on the average or gravity load demand than on the transient component of the axial load.
3. **Slenderness** – The slenderness of the column has a significant effect on the plastic rotation capacity of the section. This parameter should be included as a factor on plastic rotation capacity but should be kept separate from  $P_{cl}$  for clarity.

Table 9-6 of ASCE 41 currently reports plastic rotation capacity as a function of  $R_p$ . The plastic rotation limits should be reported in radians similar to many of the other element types in Table 9-6 of ASCE 41 and not as  $R_p$ . The use of  $R_p$  for column capacity can lead to counter intuitive results. The use of plastic rotations in radians will lead to more transparent and easily interpretable results.

#### *Additional Recommended Research*

Additional column test results from those discussed herein should be consulted/compiled for inclusion in the proposed changes to Table 9-6 of ASCE 41. Ideally, enough data points can be gathered such that the backbones outlined Table 9-6 of ASCE 41 can be realigned with 90<sup>th</sup> percentile values for the acceptance criteria and with 50<sup>th</sup> percentile values for modeling criteria. This realignment will provide consistency within the ASCE 41 document and the direction that the Concrete provisions are proposing to adopt for the 2017 update. Additionally, further investigation into the plastic rotation capacities of columns with low axial load should be conducted. Newell illustrated that ASCE 41 is potentially un-conservative for these columns and a maximum plastic rotation equal to that of an equivalent steel beam is more appropriate. Finally, additional correlation studies upon the multi-dimensional stability parameter presented in Figure 6 should be conducted that incorporate influence from axial load. Efforts to determine a universal relationship between this parameter and plastic rotation capacity should be made to investigate the potential of creating a closed form solution.

## **CONCLUSIONS**

From review of the column performance of the archetype high-rise buildings it is clear that the current force-controlled criteria in ASCE 41-13 limit the capacity of these structures. Research presented illustrates that current force-controlled criteria are conservative for high axial load. As shown, most of the columns in the Archetype buildings are acceptable when evaluated against the plastic rotation limits in NZS 3404. To avoid un-necessary and costly retrofit solutions for these types of buildings the column acceptance criteria in ASCE 41-13 should be updated. The following recommendations are provided for next steps:

1. Develop a technical ballot proposal for submission to the ASCE 41-17 Committee outlining proposed revisions to Table 9-6 that document suggested modeling and acceptance criteria. Criteria shall be developed to demonstrate conformance with Type 1 and Type 2 backbone curves per ASCE 41.
2. Re-evaluate the case study buildings using the proposed acceptance criteria illustrating the degree of conservatism in ASCE 41-13 and the potential saving to building owners on seismic retrofit costs.

## REFERENCES

- ASCE 41-13, – *Seismic Evaluation & Retrofit of Existing Buildings*, American Society of Civil Engineers, 2013.
- Allen Nudel, Masume Dana, Lindsey Maclise (2013), *Adaptive Reuse: Creating a new school of Dentistry in an Outdated Urban Office Building*, SEAOC 2013 Convention Proceedings
- ASTM MNL41 Fracture and Fatigue Control in Structures, third edition, Barsom Rolfe
- Maps of Quaternary Deposits and Liquefaction Susceptibility in the Central San Francisco Bay Region, California*, Published by the USGS in cooperation with the CGS, 2006.
- Brownlee, Scott Alexander (1994), *Axial Load and Plate Slenderness effects on the Inelastic Behavior of Structural Steel Beam-Columns*, 1994
- Harris John L. III, Spiecher Matthew S. (2015), NIST Technical Note 1863-1, Assessment of First Generation Performance Based Seismic Design Methods for New Steel Buildings, Volume 1: Special Moment Frames.
- Kelly, T.E. (2010), *Performance Based Evaluation of Buildings: Nonlinear Pushover and Time History Analysis: Reference Manual Parts 1 – 4* (aka *ANSR Reference Manual*), Holmes Consulting Group, Revision 7, September, 2010.
- MacRae, G.A. (1989). *The seismic Response of Steel Frames*, University of Canterbury Christchurch New Zealand.
- Mondkar, D.P. and Powell, G.H. (1979), *ANSR II Analysis of Non-linear Structural Response User's Manual*, EERC 79/17, University of California, Berkeley, July, 1979.
- Newell (2008). *Cyclic Behaviour and Design of Steel Columns Subjected to Large Drift*. Dissertation, UCSD, 2008.
- NISTIR 5944 Failure Analysis of Welded Steel Moment Frames Damaged in the Northridge Earthquake.
- NZS 3404: 1997, *New Zealand Steel Structures Standard*, Standards New Zealand, 1997.
- Popov, E., Bertero, V., Chandramouli, S. (1975), *Hysteretic Behavior of Steel Columns* Earthquake Engineering Research Center Report No. 75-11, 1975.
- Uang, C.M., Ozkula, G., Harris, J. (2015), *Observations from Cyclic Test on Deep, Slender Wide-Flange Structural Steel Beam-Column Members*. Proc. of Annual Stability Conference, Tennessee, Nashville, March 24-27, 2015.

## UCSF Clinical Sciences Building: Seismic Rehabilitation Case Study

Mason Walters<sup>1</sup>; Steve Marusich<sup>1</sup>; Carlos Sempere<sup>1</sup>; and Ryan Cooke<sup>1</sup>

<sup>1</sup>Forell/Elsesser Engineers, 160 Pine St., Suite 600, San Francisco, CA 94111.  
E-mail: [m.walters@forell.com](mailto:m.walters@forell.com); [s.marusich@forell.com](mailto:s.marusich@forell.com); [c.sempere@forell.com](mailto:c.sempere@forell.com);  
[r.cooke@forell.com](mailto:r.cooke@forell.com)

### Abstract

The seismic renovation of the historic 1932 Clinical Sciences Building on the UCSF Parnassus Campus will be examined. When the renovation is complete, the seven story steel framed structure with board-formed concrete façade will serve as functionally critical office space for the Moffitt Hospital staff. Because of the linkage with the hospital UCSF mandated that higher than seismic performance be achieved, but at a cost similar to conventional construction. The retrofit concept selected uses cast-in-place post-tensioned concrete shear walls with external buckling restrained brace dampers. The scheme was selected on a “Best Value” basis after evaluating several schematic-level designs. The paper will emphasize:

- Development of the project-specific design criteria.
- Application of nonlinear response history analysis techniques.
- Performance-based detailing of articulation joints between walls & floors.
- Seismic interface considerations related to adjacent buildings.

### INTRODUCTION

The Clinical Sciences Building (CSB) is located on the University of California, San Francisco (UCSF) Parnassus Heights Campus along Parnassus Avenue. It is approximately 8 kilometers from the San Andreas Fault and 22 kilometers from the Hayward Fault, leaving it susceptible to significant ground shaking from earthquakes with a range of magnitudes. Figure 1 shows the site plan for CSB and surrounding area.

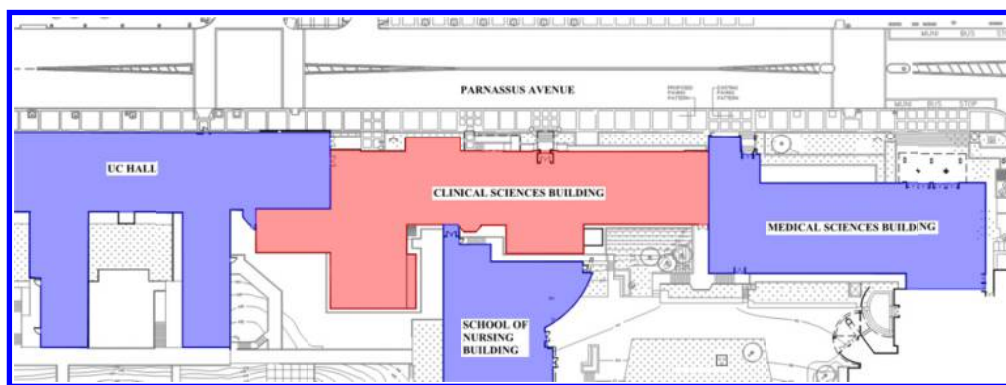
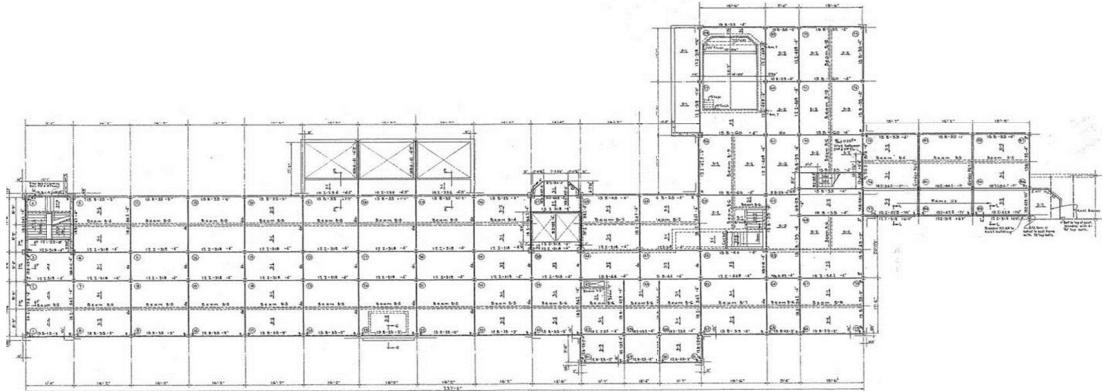


Figure 1: CSB Site Plan

CSB was originally constructed in 1932 and has undergone various renovations over the years. The building is seven stories tall with an approximate gross area of 108,000 square feet. The building has approximate overall plan dimensions of 280 feet by 100 feet and rises 100 feet above Parnassus Avenue. The structure is composed of 4 inch one-way concrete slabs supported on a complete steel frame and spread footings. The steel beams are riveted to the columns forming partially-restrained moment connections. Figure 2 shows a typical floor plan.



**Figure 2: Typical Floor Plan**

The façade is a cast-in-place board-formed concrete pier and spandrel system, see Figure 3. The structure is keyed into the adjacent hillside with an approximate two story elevation change between Parnassus Avenue and the south side of the building. Lateral loads are resisted primarily by the concrete façade and partially restrained moment connections of the steel gravity frame.



**Figure 3: North Elevation along Parnassus Avenue**

CSB is surrounded by three other structures; UC Hall to the west, Medical Sciences Building (MSB) to the east, and the School of Nursing to the south. Hallways currently connect circulation through the buildings. Although these other buildings are not attached to CSB, the physical gaps between them range from only 2 inches at the School of Nursing to about 6 inches at MSB and UCH.